Published in final edited form as:
Dev Dyn. 2015 March ; 244(3): 444–456. doi:10.1002/dvdy.24221.

microRNA-dependent Temporal Gene Expression in the Ureteric Bud Epithelium during Mammalian Kidney Development

Vidya K. Nagalakshmi[1], **Volkhard Lindner**[2], **Andy Wessels**[3], and **Jing Yu**[1,†]

[1]Department of Cell Biology, University of Virginia School of Medicine, Charlottesville, VA 22903

[2]Center for Molecular Medicine, Maine Medical Center Research Institute, Scarborough, ME 04074

[3]Regenerative Medicine and Cell Biology, Medical University of South Carolina, Charleston, SC 29425

Abstract

Background—Our previous study on mouse mutants with the ureteric bud (UB) epithelium-specific *Dicer* deletion (*Dicer* UB mutants) demonstrated the significance of UB epithelium-derived miRNAs in UB development.

Results—Our whole-genome transcriptional profiling showed that the *Dicer* mutant UB epithelium abnormally retained transcriptional features of the early UB epithelium and failed to express many genes associated with collecting duct differentiation. Further, we identified a temporal expression pattern of early UB genes during UB epithelium development in which gene expression was detected at early developmental stages and became undetectable by E14.5. In contrast, expression of early UB genes persisted at later stages in the *Dicer* mutant UB epithelium and increased at early stages. Our bioinformatics analysis of the abnormally persistently expressed early genes in the *Dicer* mutant UB epithelium showed significant enrichment of the *let-7* family miRNA targets. We further identified a temporal expression pattern of *let-7* miRNAs in the UB epithelium that is anti-parallel to that of some early UB genes during kidney development.

Conclusions—We propose a model in which the *let-7* family miRNAs silence the expression of a subset of early genes in the UB epithelium at later developmental stages in order to promote collecting duct differentiation.

Keywords

miRNAs; let-7; mouse; collecting duct differentiation

Introduction

During metanephric kidney development, the highly proliferative ureteric bud (UB) epithelial cells undergo branching morphogenesis and differentiate to form a functional collecting duct tree of the kidney. The UB epithelium is composed of the UB tip and UB

[†]Corresponding author: Jing Yu, Department of Cell Biology, University of Virginia School of Medicine, Charlottesville, VA 22908, Phone: 434-982-0203, Fax: 434-982-3912, jy4m@virginia.edu.

trunk epithelium. The UB tip cells are stem cells that give rise to UB trunk cells and also self-renew to generate more UB tip cells until P4–P6 in mice (Rumballe et al., 2011; Shakya et al., 2005). The UB trunk cells proliferate to make more UB trunk cells (Shakya et al., 2005) and differentiate into the collecting duct epithelium starting at around E15.5 (Marose et al., 2008). Thus, the UB tip and trunk epithelium constitute the precursor cell population for the future collecting duct epithelium of the developing metanephros. The collecting duct epithelium comprises primarily of two cell types, principal cells and intercalated cells, which are distinct in their structure and function (Bagnis et al., 2001). The renal collecting duct system plays a critical role in regulating body water and salt homeostasis and the acid-base balance. Therefore, proper collecting duct differentiation from the UB epithelium precursors during embryonic and fetal development is vital for renal function. Previous experimental evidence reveals that β-catenin-mediated signaling in the UB epithelium and Heregulin of the mesenchyme contribute to the transition of UB epithelial cell fate from the precursor to the differentiated fate (Marose et al., 2008; Sakurai et al., 2005). In addition, Notch signaling and transcription factor *Foxi1* contribute to the UB epithelial cell fate choices between principal and intercalated cells (Blomqvist et al., 2004; Guo et al., 2014; Jeong et al., 2009). A role of epigenetic mechanisms in UB epithelial cell fate choices is also evident, as loss of *Dot1l*, a H3K79 methyl transferase, in principal cells leads to their transition to the intercalated cell fate (Wu et al., 2013).

Non-coding RNAs such as microRNAs (miRNAs) are known as molecular rheostats for modulating their target gene expression to promote cell fate changes and cell differentiation (Wu et al., 2009). In fact, miRNAs were first discovered through *C. elegans* heterochronic mutants, in which *lin-4* and *let-7* miRNAs were found to regulate the timing of distinct developmental events during the progression of larval to adult stages in worms (Ambros, 2011). In adult or tissue-specific stem cells, miRNAs have been demonstrated to regulate the transition of highly proliferating and self-renewing progenitor cell fate to a terminally differentiated cell fate in several systems including neuronal tissues, skeletal and cardiac muscle tissues, skin and airway bronchial epithelial cells, and also in hematopoiesis (Akerblom and Jakobsson, 2013; Fazi and Nervi, 2008; Follert et al., 2014; Gangaraju and Lin, 2009; Ghosh et al., 2014; Johanson et al., 2014; Lize et al., 2011). In addition, the overall significance of the miRNA pathway in cell differentiation has been deduced from the compromised differentiation of *Dicer* and *DGCR8* deficient embryonic stem (ES) cells both *in vitro* and *in vivo* (Chen et al., 2010; Gangaraju and Lin, 2009) and from defective osteoclast differentiation and function resulting from disruption of the *Dicer*-regulated miRNA biogenesis pathway (Sugatani and Hruska, 2009). Deregulation of miRNAs has also been associated with the cell fate changes implicated in tumorigenesis and cancer initiation (Chao et al., 2014; Morris et al., 2014).

The role of one of the miRNA families, the *let*-7 family, in promoting cell differentiation has been widely studied and has been proved in several organ systems (Ambros, 2011; Bao et al., 2013; Bussing et al., 2008; Copley and Eaves, 2013; Meza-Sosa et al., 2014; Roush and Slack, 2008; Sokol, 2012). A conserved role of the *let-7* family miRNAs is to suppress early cell fate regulators and promote cell differentiation as development continues. As stated earlier, *let-7* was one of the first miRNAs identified that regulate developmental timing in *C.*

elegans (Ambros, 2011). *let-7* is undetectable in human and mouse embryonic stem cells, and its expression levels increase during differentiation. One of the *let-7* targets, *Lin28* (Ambros, 2011), which is also critically involved in the heterochronic pathway in *C. elegans*, has been used as a reprogramming factor to derive induced pluripotent stem cells (iPSCs) (Yu et al., 2007). Further, during reprogramming of differentiated cells into iPSCs, the *let-7*-based pathway has been observed to counteract the activity of reprogramming factors by promoting the expression of pro-differentiation genes (Worringer et al., 2014). The *let-7* family members have also been shown to play a critical role in lineage specification during neural differentiation in the developing brain of mouse embryos (Meza-Sosa et al., 2014; Wulczyn et al., 2007) and have also been implicated as key regulators of the early to late developmental transition in retinal progenitors (La Torre et al., 2013). In human erythroid cells and hematopoietic organs, *Lin28b*-mediated suppression of *let-7* regulates the fetal-to-adult developmental transition of erythroblasts (Lee et al., 2013). Also, in mouse adult fibroblasts, *let-7* miRNAs suppress the expression of a mid-gestation developmental program representing a period between the pluripotent state at E3.5 and differentiation at E10.5 (Gurtan et al., 2013). Studies have also shown that developmental dysregulation of *let-7*-mediated gene expression leads to the onset of cancer and tumorigenesis (Boyerinas et al., 2010).

In our previous studies with UB-specific *Dicer* mutant mice (*Dicer* UB mutants), we demonstrated the critical role of miRNAs of the UB lineage in UB branching morphogenesis and collecting duct tube size control and differentiation (Nagalakshmi et al., 2011). In the current study we aimed to define the miRNA-regulated transcriptional changes in the *Dicer* UB mutants. Our current study identified a novel phenomenon of miRNA-mediated temporal restriction of gene expression in the UB epithelium during kidney development. In addition, we substantiated and further extended our previous finding that *Dicer*-mediated miRNA-regulated pathways are critical in the early to late cell fate transition in the UB epithelium that allows normal collecting duct differentiation. Moreover, we identified a temporal expression pattern of the *let-7* family miRNAs in the UB epithelium that inversely correlates with that of some early UB genes, including their putative target genes.

Results

Microarray analysis identified 143 miRNAs expressed in the E15.5 UB epithelium

Though several earlier studies defined the critical roles of UB-expressed miRNAs in kidney development (Bartram et al., 2013; Nagalakshmi et al., 2011; Pastorelli et al., 2009; Patel et al., 2012; Patel et al., 2013), it is still not known which miRNAs are expressed in the UB epithelial cells. Given the importance of this information for understanding how UB-derived miRNAs regulate kidney development and also for validating the cognate miRNAs of the dysregulated target genes in E15.5 *Dicer* mutant UB epithelium (see below), we performed miRNA microarray analysis on FACS-sorted E15.5 wild-type (WT) UB epithelial cells labeled with YFP by crossing a Rosa26YFP Cre reporter (Srinivas et al., 2001) with the *Hoxb7Cre* driver line (Yu et al., 2002). The miRNA array data have been deposited at NCBI-Gene Expression Omnibus (GEO-GSE60845). Our analysis revealed a significant presence of 143 miRNAs (signal >32) in the E15.5 UB epithelium.

Transcriptional profiling with *Dicer* UB mutants

Our previous studies with the *Dicer* UB mutants revealed the critical role of miRNAs in UB epithelial morphogenesis and differentiation during kidney development (Nagalakshmi et al., 2011). miRNAs function through inhibition of their target genes. Therefore, to understand how UB-expressed miRNAs regulate UB development, we set forth to identify potential miRNA targets in the UB epithelium. The UB epithelial cells were specifically labeled with YFP by crossing a Rosa26YFP Cre reporter into the *Dicer* UB mutant (*Dicer*$^{C/-}$*; HoxB7Cre*) and control backgrounds and then FACS-sorted at E15.5. We chose this developmental stage for transcriptional profiling because the hypoplastic and cystic defects have just become obvious in the *Dicer* UB mutants at this stage (Nagalakshmi et al., 2011), and differentiation of the collecting ducts, at least in terms of the transcription of differentiation markers, becomes significant at around this stage. In addition, the branching defect of *Dicer* mutant UB epithelium remained at E15.5 (Nagalakshmi et al., 2011). Thus, this stage provides an ideal setting for comparing the normal and mutant UB epithelium for changes in gene expression regulating all three defects observed in the *Dicer* mutant UB epithelium, namely, defects in UB branching morphogenesis, UB epithelial differentiation, and collecting duct tube size determination. Transcriptional profiling of both *Dicer* mutant and control UB cells was performed with Affymetrix Whole Transcript Gene 1.0 ST Arrays. This analysis identified 679 genes upregulated in mutants by 1.5 fold or more ($p<0.05$) and 440 genes downregulated by 1.5 fold or more ($p<0.05$). The number of upregulated genes was greater than the number of downregulated genes, and this is consistent with the fact that miRNAs are generally negative regulators of their targets. The microarray data have been deposited at GEO (GSE60758). Pathway analyses including Gene Ontology Overrepresentation Analysis (GO), Gene Set Enrichment Analysis (GSEA), and Signaling Pathway Impact Analysis (SPIA) revealed that the differentially regulated genes in the *Dicer* mutant UB epithelium were not significantly enriched for any annotated pathways.

Dicer removal disrupted collecting duct differentiation and abnormally retained the UB epithelium at an early stage of development

We then subjected the differentially regulated genes in the *Dicer* mutant UB epithelium to ToppGene analysis (https://toppgene.cchmc.org). Remarkably, this analysis revealed that the upregulated genes in *Dicer* mutants at E15.5 were enriched with E10.5 UB epithelial genes ($p=4.86\times10^{-17}$), E10.5 being the earliest time point when the UB epithelium begins to form (Table 1). Conversely, the downregulated genes in the *Dicer* UB mutants were enriched for E15.5 medullary collecting duct genes ($p = 2.39\times10^{-25}$) (Table 2), which included some of the published markers associated with principal and intercalated cells such as *Foxa1, Aqp3, Rnf186, Avpr2, Kcnq1,* and *Gsdmc* (Ma et al., 2000; Nonoguchi et al., 1995; Yu et al., 2012; Zheng et al., 2007). This unbiased analysis strongly indicates that in the absence of *Dicer*, the E15.5 UB cells abnormally retained the UB cell identity of early developmental stages and failed to differentiate into either principal or intercalated cells properly, substantiating and extending our previous finding of defective collecting duct differentiation of the *Dicer* mutant UB epithelium based on selected marker analysis (Nagalakshmi et al., 2011). Of note, the expression of *Aqp6* and *Nos1*, two markers that we previously showed to be reduced in expression in *Dicer* UB mutants at P0 (Nagalakshmi et al., 2011), were also

reduced in the *Dicer* mutant UB epithelium at E15.5, but they were not included in this analysis (Table 2) because their change (decreased by 1.2 and 1.3 fold, respectively) was below our cutoff (1.5 fold or greater).

miRNAs mediate temporal gene expression during UB epithelial development

The upregulated genes in the UB epithelium of E15.5 *Dicer* UB mutants shared more E10.5 than E15.5 wild-type UB transcriptional features, suggesting that during normal UB development, the expression of a subset of genes is subject to temporal regulation such that the genes are expressed during the early stages (E10.5) and silenced at later stages of development (E15.5). Indeed, examination of gene expression profiles of isolated UB and collecting duct cells from wild-type kidneys in the GUDMAP database (www.gudmap.org) clearly showed that most of the genes in Table 1 have higher levels of expression in the E10.5 or E11.5 UB than in E15.5 collecting ducts, especially E15.5 medullary collecting ducts. Further, the transcription profiling comparison of control and *Dicer* mutant UB cells implies that miRNA-regulated pathways mediate this temporal regulation of gene expression. We set forth to verify and test both notions by examining the temporal mRNA expression pattern in the control and *Dicer* mutant UB epithelia of 4 genes randomly selected from Table 1, *Cthrc1*, *Hapln1*, *Ptprz1*, and *Lin28b*, at E11.5–E15.5 with *in situ* hybridization (Fig. 1).

As shown in Fig. 1, in control kidneys, all 4 genes were detected in the UB epithelium at E11.5. *Cthrc1*, *Hapln1*, and *Lin28b* were also expressed in the UB epithelium at E12.5 and E13.5, but *Ptprz1* expression in the UB epithelium was undetectable at these stages. At E14.5 and E15.5, none of the 4 genes was detected in the UB epithelium, though *Cthrc1*, *Hapln1*, and *Lin28b* were expressed in non-UB structures. These data confirmed that the expression of these genes in the UB epithelium is temporally regulated during normal development, and that their expression is associated with early UBs. We have referred to genes that are expressed in the UB epithelium only at early developmental stages as early UB genes for simplicity.

In contrast to the control situation, persistent expression of these four genes throughout the stages examined was observed in the UB epithelium of the *Dicer* UB mutants (Fig. 1), and at the stages when they were expressed in the control littermates, their expression in the mutant UBs appeared stronger, at least at E12.5 and E13.5. This indicates that *Dicer*-dependent miRNAs are required for the regulation of temporal expression of these genes, by suppressing their expression more dramatically at later developmental stages.

An early, cell-autonomous, branching defect in *Dicer* UB mutants

We have observed UB branching defects as early as E13.5 in our previous analysis of *Dicer* UB mutants (Nagalakshmi et al., 2011). As our current study showed deregulation in the expression of early UB genes before E13.5 in the UB epithelium of the *Dicer* UB mutants (Fig. 1), we set forth to determine whether the branching defect also occurred prior to E13.5. Visualization of the UB network with GFP fluorescence from the Cre reporter $Rosa^{mT/mG}$ (Muzumdar et al., 2007) revealed that the first branching event at E11.5 was normal for mutant kidneys. In contrast, a significant defect in UB branching was clearly observed in the

mutants at E12.5, where fewer branch tips were present (Fig. 2). Further, mesenchyme-free UBs dissected from E11.5 kidneys and cultured in matrigel supplemented with GDNF and retinoic acid also showed a significant reduction in branching of the *Dicer* mutant UBs compared to their control littermates within 24 hours in culture (Fig. 3). This result indicates that UB branching defects observed in the *Dicer* UB mutants are cell-autonomous, and that the *Dicer*-ablated UB epithelium was significantly compromised in its intrinsic ability to respond to mesenchymal branching signals early on during kidney development.

The role of early UB genes in UB epithelial morphogenesis

In order to understand the functional significance of the early UB genes that were upregulated in the E15.5 UB epithelium of the *Dicer* UB mutants, we examined the mouse null mutant kidneys for two of the early UB genes, *Cthrc1* and *Hapln1*. The UB epithelium undergoes active branching events during the early stages of kidney development until E14.5 and branching morphogenesis slows down thereafter (Cebrian et al., 2004; Short et al., 2014), so one possibility is that temporal genes expressed in the early UB epithelium facilitate the early rapid branching events during kidney development. Alternatively or additionally, early UB gene expression in the UB epithelium maintains its undifferentiated precursor fate, as demonstrated for canonical Wnt signaling in the UB epithelium (Marose et al., 2008). In either scenario, branching morphogenesis is expected to decrease when the expression of early UB genes is ablated from the UB epithelium, with the decrease resulting from the failure to sustain rapid branching at the early developmental stages, and/or from premature differentiation of the UB epithelium. However, our examination of the *Cthrc1* and *Hapln1* null mutants revealed no significant difference in branching morphogenesis or collecting duct formation between the null mutants for *Cthrc1* and *Hapln1* and their control littermates (Fig. 4). It could be that *Cthrc1* and *Hapln1* are not required for early UB development. Alternatively, it may be that several temporal genes act redundantly to regulate UB development, and deletion of just one gene is not sufficient to produce a discernible effect. Compound mutants of multiple early UB genes or ablation of common upstream regulators, if any, should address this possibility in the future.

Inversely correlated temporal expression pattern of the *let-7* family of miRNAs with early UB genes during UB development

Given the nature of miRNA regulation of their targets and the above observation that miRNAs were required for repression of some early UB gene expression in the UB epithelium at later developmental stages, it is very possible that some of the early UB genes in Table 1 are direct targets of miRNAs that are expressed only, or at higher levels, at later developmental stages. Identification of the miRNAs that directly target early UB genes is crucial for understanding the functional significance of, and the mechanisms underlying, the temporal regulation of UB development. We therefore applied ToppGene analysis to early UB genes in Table 1 to identify miRNAs that potentially target these genes. Strikingly, this analysis revealed that these early UB genes, which were abnormally persistently expressed in the E15.5 UB epithelium of the *Dicer* mutants, were most significantly enriched for putative targets of the *let-7* family of miRNAs (Table 3). Sixteen genes in Table 1 were predicted as *let-7* family miRNA targets (Table 4), including *Cthrc1* and *Lin28b*, the temporal expression of which in the UB epithelium was validated in the present study (Fig.

1). Our miRWalk analysis with 10 miRNA target prediction algorithms also verified that 13 of the 16 mouse genes (except *Clcn5*, *Cdkn1a*, and *Ly75*) are putative *let-7* miRNA targets. Out of the 13 predicted *let-7* target early UB genes, at least three of them, *Igf2bp1*, *Prtg*, and *E2f5*, have been validated as direct *let-7* targets through reporter assays in earlier studies (Cheng et al., 2013; La Torre et al., 2013; Papaioannou et al., 2013).

The vertebrate genome encodes 10 *let-7* family mature miRNAs (miRBase-Version 21), which share the seed sequence and therefore target genes. Our miRNA microarray analysis with FACS-sorted wild-type UB epithelial cells from E15.5 kidneys revealed the presence of 8 out of 10 *let-7* family members at significantly high levels (Table 5). Further, our previous study with miRNA *in situ* hybridization confirmed the expression of one of the members, *let-7a*, in the E15.5 control UB epithelium and demonstrated a great reduction in its expression in the *Dicer* mutant UB (Nagalakshmi et al., 2011). We further examined the temporal expression pattern of these 8 *let-7* family miRNAs in the wild-type UB epithelium during kidney development with qRT-PCR analysis. The 8 *let-7* miRNAs were expressed in the UB epithelium at all the stages examined, but the expression levels of all of them increased significantly in the UB epithelium at later stages of E14.5 and E15.5 compared to that of the early stages of E11.5 and E12.5 (Fig. 5). Therefore, the temporal expression pattern of *let-7* family members in the UB epithelium during kidney development is inversely correlated to the expression of some of the early UB genes, including the putative *let-7* targets *Cthrc1* and *Lin28b* (Fig. 1). The expression of *let-7* family miRNAs at early stages of UB development, though at lower levels, offers an explanation of the increased expression levels of early UB genes at these stages in *Dicer* UB mutants.

Discussion

miRNAs regulate a myriad of biological processes in living organisms. The critical regulatory functions of miRNAs in kidney development and disease is underscored by the experimental evidence of the presence of miRNA-mediated gene regulation in the kidneys, as well as the defective kidney phenotypes observed in several studies in which the global miRNA biogenesis pathway or the expression of individual miRNAs is compromised. Our earlier phenotypic analyses on the *Dicer* UB mutants revealed the significance of miRNA-regulated pathways in UB branching and in collecting duct tube size determination and terminal differentiation (Nagalakshmi et al., 2011). The present study further substantiates and extends the scope of *Dicer*-dependent miRNAs in regulating UB epithelial cell fate during developmental progression. In addition, it illuminates a miRNA-dependent temporal expression pattern of early UB genes in the UB epithelium during embryonic development and implicates the *let-7* family miRNAs in this regulation.

Temporal expression of early UB genes in the UB epithelium during kidney development

Our bioinformatics and *in situ* hybridization analyses showed that during UB development, a group of genes, which we refer to as early UB genes, are present in the UB epithelium at early stages of development and undetectable during the later stages (Fig. 1). Similar temporal changes in the UB epithelium were reported before for canonical Wnt activity (Iglesias et al., 2007; Jho et al., 2002; Maretto et al., 2003) and *Sall4* expression (Toyoda et

al., 2013) in the developing UB trunks. The present study shows that this is not a rare phenomenon in UB development; rather, the expression of a significant group of genes is silenced later in embryonic UB development. It is worth noting that the number of early UB genes is most likely larger than that in Table 1, as our analysis focused only on genes whose expression was upregulated from the loss of *Dicer*. It is very likely that the temporal expression of some early UB genes is not under the control of *Dicer*-dependent miRNAs. Additionally or alternatively, not all early UB genes whose temporal expression is regulated by *Dicer*-dependent miRNAs were upregulated, or upregulated by at least 1.5 fold, in *Dicer* mutants, given the complex changes in the UB epithelium resulting from the loss of over a hundred miRNAs when *Dicer* was removed. Indeed, the expression of *Sall4* and canonical Wnt readouts *Lef1* and *Axin2*, which are expressed only in the early UB epithelium, were reduced in *Dicer* mutant UBs.

Our *in situ* hybridization of 4 randomly selected early UB genes showed that there are two different temporal patterns. While the expression of *Cthrc1*, *Hapln1*, and *Lin28b* in the UB epithelium started to become undetectable starting at E14.5, *Ptprz1* expression in the UB was only detected at E11.5. Interestingly, *Sall4* has a temporal expression pattern similar to that of *Ptprz1*, where it is strongly expressed in the UB epithelium at E11.5 but very weakly expressed at E12.5 and not detected to be expressed by E13.5 (Toyoda et al., 2013). These data strongly suggest that the regulation of temporal expression of early UB genes is complex and likely involves different molecular players/mechanisms.

The *let-7* family miRNAs and UB epithelial cell fate change

ToppGene analysis was used to compare the genes in E15.5 *Dicer* UB mutants downregulated by 1.5 fold or more with GUDMAP transcription profiling data generated from the collection of wild-type renal cell populations of various developmental stages. The downregulated transcripts of *Dicer* mutants were observed to be enriched for genes expressed in the E15.5 medullary collecting ducts, the only representation of differentiated collecting ducts in the GUDMAP database. Therefore, our whole transcriptome analysis revealed a clear defect in collecting duct differentiation from the UB precursors with *Dicer* removal.

How do *Dicer*-dependent miRNAs regulate UB epithelial cell fate changes and promote collecting duct differentiation? The inverse correlation of the temporal expression pattern of the *let-7* family miRNAs and their putative early UB target genes in both the normal and *Dicer* mutant UB epithelium is consistent with the model that *let-7* miRNAs suppress the expression of their putative target genes and potentially some other early UB genes secondarily in the UB epithelium at later stages of development (Fig. 6). The *let-7* family miRNAs have been associated with temporal progression of development and cell differentiation in multiple organisms and tissue types (Ambros, 2011; Bao et al., 2013; Bussing et al., 2008; Copley and Eaves, 2013; Meza-Sosa et al., 2014; Roush and Slack, 2008; Sokol, 2012). In the kidney, the *let*-7 miRNA has been implicated in the decision between self-renewal and differentiation of nephron progenitors (Urbach et al., 2014). It is possible that the *let-7* family miRNAs are required for proper differentiation of the UB epithelium into the collecting ducts, by suppressing early UB genes at later developmental

stages, directly and/or through *let-7* miRNA target genes (Fig. 6). Thus, in the absence of the *let-7* family miRNAs, as in the case of *Dicer* UB mutants, early UB gene expression fails to be repressed in the later-stage UB epithelium, thereby maintaining the UB epithelium in an early state which obstructs collecting duct differentiation. In addition, the upregulated expression of early UB genes, including some of the *let-7* targets, during early stages of UB development (Fig. 1; Table 4) may also interfere with the normal branching pattern as observed in the *Dicer* mutants (Fig. 2 and 3), similar to the case of constitutive activation of Wnt/β-catenin signaling in the UB epithelium (Marose et al., 2008).

The mechanisms that maintain ureteric bud epithelial cells in the precursor state and that promote them to collecting duct differentiation are little understood. Heregulin from the mesenchyme was previously shown to promote collecting duct differentiation in kidney culture (Sakurai et al., 2005), and Wnt/β catenin signaling in the UB epithelium promotes/maintains its precursor state (Marose et al., 2008). Our current study suggests another layer of regulation, operated by miRNAs, in the cell fate decision during UB epithelium development. Future work establishing the role of *let-7* family miRNAs in UB epithelial differentiation and the molecular regulators involved in this process will provide further understanding of the mechanisms by which the UB epithelial cells transition from the precursor state to the differentiated state. In the long run, these findings should facilitate development of effective strategies to maintain the UB epithelial cells in a precursor state and to differentiate collecting duct cells *in vitro* for cell-based therapies to repair the collecting duct system in damaged/disease kidneys.

Experimental Procedures

Mice

The conditional *Dicer* ureteric bud mutants (*Dicer*$^{C/-}$*; HoxB7Cre*) were generated as described previously (Nagalakshmi et al., 2011). Three fluorescent reporter mouse lines were used in the study. The UB epithelial cells were specifically labeled with YFP for fluorescence-activated cell sorting (FACS) by crossing a Rosa26YFP Cre reporter (Srinivas et al., 2001) into the *Dicer*$^{C/-}$*; HoxB7Cre* and control backgrounds. Wild-type UB epithelial cells were sorted from *HoxB7/*Myr-venus mice (Chi et al., 2009). For whole-mount kidney imaging, the *Rosa*$^{mT/mG}$ mice (Muzumdar et al., 2007) were crossed into the *Dicer*$^{C/-}$*; HoxB7Cre* and control backgrounds. The mouse null mutants for *Cthrc1* (*Cthrc1*$^{-/-}$) and *Hapln1* (*Crtln1*$^{-/-}$) were generated as described previously (Stohn et al., 2012; Watanabe and Yamada, 1999). All experimental procedures performed with mice were in accordance with institutional and national guidelines, policies, and animal welfare laws, and were approved by the institutional animal care and use committee.

Tissue preparation

Tissue preparation for immunofluorescence staining and *in situ* hybridization was done as previously described (Nagalakshmi et al., 2011). Briefly, to prepare frozen blocks, kidneys were fixed in 4% paraformaldehyde (PFA) and then cryopreserved in 30% sucrose before being embedded in OCT medium. For whole-mount tissue preparation, tissues were fixed in 4% PFA for 1 h at 4°C for immunostaining, and for 24 h at 4°C for *in situ* analysis. After

fixation, tissues were immunostained or were dehydrated with a graded series of methanol/0.85%NaCl and were stored in 100% methanol for *in situ* hybridization analysis.

In situ hybridization

In situ hybridization analysis was performed on whole-mount kidneys as well as on sections from frozen blocks following protocols previously described (Nagalakshmi et al., 2011). Tissue were hybridized with the antisense probes for *Hapln1* (*Crtln1*), *Cthrc1*, *Ptprz1*, and *Lin28b* with whole-mount kidneys for E11.5 and 16 μm frozen sections for E12.5–E15.5. DNA templates for riboprobe synthesis were generated by polymerase chain reaction (PCR) from total embryonic kidney cDNAs. The sense and the antisense gene-specific primers were linked at the 5′ ends to T3 and T7 polymerase promoter sequences, respectively. The amplified gene product was verified by sequencing. Digoxigenin-labeled RNA probes were synthesized using the Roche Dig RNA labeling mix (Roche 1277073). The primers used in the current study were:

Cthrc1-Sense: AATTAACCCTCACTAAAGGGCTGCTGCTCGGTCTCTTCCT

Antisense: TAATACGACTCACTATAGGGTCGGTAGTTCTTCAATGATGATG

Hapln1-Sense:
AATTAACCCTCACTAAAGGGTGTGGAAGCAGAACAAGCCAAG

Antisense: TAATACGACTCACTATAGGGTTGCACCGCCTCATCGTAGGT

Ptprz1-Sense: AATTAACCCTCACTAAAGGGCCACTGAAGATGCCGAACTTG

Antisense: TAATACGACTCACTATAGGGTGATTCCTCTGAACCTGATGG

Lin28b-Sense:
AATTAACCCTCACTAAAGGGCAAGCAAAGGTGAAGAGCCAGA

Antisense: TAATACGACTCACTATAGGGTGACCTGTCTGAGTGCTCTGC

Immunostaining

Immunostaining was performed on whole-mount kidneys as well as on sections from frozen blocks following protocols described previously (Nagalakshmi et al., 2011). Briefly, whole-mount kidneys were permeabilized with tsPBS (0.5% Triton and 0.1% saponin in phosphate buffered saline [PBS]) at 4°C overnight and then incubated in blocking buffer (3% BSA, 1% normal donkey serum, 0.1% Triton X-100/PBS) at 4°C overnight. Frozen blocks were sectioned at a thickness of 12 μm, and the sections were blocked with the blocking buffer at room temperature for 1 hour. After blocking, tissues were treated with primary and secondary antibodies diluted in the blocking buffer overnight at 4°C. Anti-pan Cytokeratin (Sigma 1:500) was used as the primary antibody. Sections post-fixed with 4% PFA for 20 minutes at room temperature were stained with Hoechst 33342 for 5 minutes and mounted with Fluoromount-G mounting media (Southern Biotech; Cat. No: 0100-01). Whole-mount kidneys post-fixed with 4% PFA for 30 minutes were dehydrated using a graded series of Methanol/0.85% NaCl and stored in 100% Methanol. Before imaging, tissues were cleared with BA:BB mixture (1:1 Benzyl alcohol and Benzyl benzoate) for better visualization.

Fluorescence-activated cell sorting (FACS)

Wild-type and mutant embryonic kidneys obtained from the fluorescent reporter cross were dissected into DPBS (Gibco) on ice. Tissues were then trypsinized with 0.05% Trypsin/EDTA (Gibco) at 37°C. Trypsinization was then quenched with the addition of DMEM (Gibco) supplemented with 10% FBS (Gibco). Single-cell suspension of the kidney was then obtained by trituration with P1000 and P200 pipette tips. The cell suspension was filtered through 70 μm cell strainers (BD Falcon) and collected in 2% BSA (Difco). YFP-positive cells were sorted using a Becton Dickinson FACS Vantage SE Turbo Sort DIVA Cell Sorter in the University of Virginia Flow Cytometry Core Facility. Sorted cells were collected in DMEM supplemented with 20% FBS, pelleted, and stored at −80°C until used for RNA preparation.

Microarrays

Total RNA was extracted from the FACS-sorted cells using an RNeasy Plus Micro Kit (Qiagen) following the manufacturer's protocol. Transcriptional profiling was done using the Affymetrix Mouse Gene 1.0 ST array platform (Affymetrix) at the University of Virginia Bioinformatics Core Facility. For each of the biological replicates, 100–150 ng of total RNA was generated from 30–45,000 UB epithelial cells, and three biological replicates were profiled for each of the control and *Dicer* UB mutant categories. All of the bioinformatics and post-array analysis was performed at the University of Virginia Bioinformatics Core Facility. All preprocessing and analysis was done using R version 3.0.0. CEL files were imported using the oligo package, and the expression intensities were summarized, normalized, and transformed using the Robust Multiarray Average Algorithm. Probesets were annotated using the Bioconductor annotation package mogene 10 st transcript cluster.db, using the annotate package. Probesets not mapping to an Entrez gene were excluded. To examine differential gene expression, a linear model was used with empirical Bayes moderated standard errors using the limma package in R (Smyth, 2004). The Bioconductor package array Quality Metrics was used to perform quality assessment on the preprocessed, summarized, normalized, transformed, filtered data. Principal component analysis, hierarchical clustering, and heatmap analysis were performed to test on the quality of the array data derived from the individual biological replicates in the wild-type and *Dicer* UB mutant categories. Genes upregulated with a fold change ≥1.5 and a False Discovery Rate (FDR) *p*-value ≤0.05 or downregulated with a fold change ≤1.5 and p-value ≤ 0.05 were considered for Gene Ontology Over representation Analysis (GO), Gene Set Enrichment Analysis (GSEA) (Subramanian et al., 2005), and Signaling Pathway Impact Analysis (SPIA) (Tarca et al., 2009).

For the miRNA microarrays, total RNA including miRNAs was prepared using a miRNeasy Mini Kit (Qiagen) from the FACS-sorted E15.5 wild-type UB epithelial cells to generate 4–4.5 μg of RNA per array; the RNA was then profiled using LC Sciences microRNA Microarrays based on Sanger miRBase version 16. Two arrays were profiled, representing two biological replicates. Array hybridization and post-analysis were done by LC Sciences. Array hybridization was done using Cy3- and Cy5-labeled probes, and the signal intensity was directly read as the miRNA expression profile. The signal values were derived by

background subtraction and normalization, and transcripts with average signal intensity above 32 were considered significantly present.

miRNA analysis with qRT-PCR

Total RNA including miRNAs was extracted using an RNeasy Plus Micro Kit (Qiagen) from UB cells sorted from E11.5–E15.5 kidneys. First-strand cDNA synthesis and quantitative PCR analysis for the *let-7* family of miRNAs (*let-7a, b, c, d, e, f, g, i*) were performed using Taqman miRNA Assays (Applied Biosystems) following the manufacturer's protocol.

Mesenchyme-free UB (iUB) organ culture

Kidneys were dissected from E11.5 embryos and ureteric buds were isolated from the surrounding mesenchyme as described previously (Costantini et al., 2011). The isolated ureteric buds were cultured in matrigel supplemented with D-MEM/F12 (Gibco) containing 10% FBS (Gibco), 200 nM cis and trans retinoic acid, and 100 ng/mL recombinant rat GDNF (as recommended by Prof. Frank Costantini's lab; personal communication). Images were taken at 24 h time intervals with a DFC300 FX camera attached to a Leica MZ16F Stereoscope.

Acknowledgments

Grant support

This work was supported by American Heart Association Grant-in-Aid 12GRNT12060070 and National Institutions of Health (NIDDK) R01DK085080 to J.Y., and Project 1233 from the South Carolina Clinical & Translational Research (SCTR) Institute, with an academic home at the Medical University of South Carolina CTSA, NIH Grant Numbers UL1RR029882 and UL1TR000062 to A.W..

This study was supported by funding from American Heart Association Grant-in-Aid 12GRNT12060070 and National Institutions of Health (NIDDK) R01DK085080 to J.Y., "South Carolina COBRE for Developmentally Based Cardiovascular Diseases", P30 GM103342-01, R01HL033756-30, and American Heart Association Grant-in-Aid 13GRNT16220004 to A.W. We are thankful to the UVA flow cytometry core facility, UVA DNA sciences core facility, UVA Bioinformatics core facilities, and Dr. Stephen Turner for their support of and assistance rendered to this study, and to Dr. Bruce Aronow, Cincinnati Children's Hospital, for assistance with ToppGene usage.

References

Akerblom M, Jakobsson J. MicroRNAs as Neuronal Fate Determinants. Neuroscientist. 2013; 20:235–242. [PubMed: 23877999]

Ambros V. MicroRNAs and developmental timing. Curr Opin Genet Dev. 2011; 21:511–7. [PubMed: 21530229]

Bagnis C, Marshansky V, Breton S, Brown D. Remodeling the cellular profile of collecting ducts by chronic carbonic anhydrase inhibition. Am J Physiol Renal Physiol. 2001; 280:F437–48. [PubMed: 11181405]

Bao MH, Feng X, Zhang YW, Lou XY, Cheng Y, Zhou HH. Let-7 in cardiovascular diseases, heart development and cardiovascular differentiation from stem cells. Int J Mol Sci. 2013; 14:23086–102. [PubMed: 24284400]

Bartram MP, Hohne M, Dafinger C, Volker LA, Albersmeyer M, Heiss J, Gobel H, Bronneke H, Burst V, Liebau MC, et al. Conditional loss of kidney microRNAs results in congenital anomalies of the kidney and urinary tract (CAKUT). J Mol Med (Berl). 2013; 91:739–48. [PubMed: 23344677]

Blomqvist SR, Vidarsson H, Fitzgerald S, Johansson BR, Ollerstam A, Brown R, Persson AE, Bergstrom GG, Enerback S. Distal renal tubular acidosis in mice that lack the forkhead transcription factor Foxi1. J Clin Invest. 2004; 113:1560–70. [PubMed: 15173882]

Boyerinas B, Park SM, Hau A, Murmann AE, Peter ME. The role of let-7 in cell differentiation and cancer. Endocr Relat Cancer. 2010; 17:F19–36. [PubMed: 19779035]

Bussing I, Slack FJ, Grosshans H. let-7 microRNAs in development, stem cells and cancer. Trends Mol Med. 2008; 14:400–9. [PubMed: 18674967]

Cebrian C, Borodo K, Charles N, Herzlinger DA. Morphometric index of the developing murine kidney. Dev Dyn. 2004; 231:601–8. [PubMed: 15376282]

Chao CH, Chang CC, Wu MJ, Ko HW, Wang D, Hung MC, Yang JY, Chang CJ. MicroRNA-205 signaling regulates mammary stem cell fate and tumorigenesis. J Clin Invest. 2014

Chen L, Wang D, Wu Z, Ma L, Daley GQ. Molecular basis of the first cell fate determination in mouse embryogenesis. Cell Res. 2010; 20:982–93. [PubMed: 20628366]

Cheng M, Si Y, Niu Y, Liu X, Li X, Zhao J, Jin Q, Yang W. High-throughput profiling of alpha interferon- and interleukin-28B-regulated microRNAs and identification of let-7s with anti-hepatitis C virus activity by targeting IGF2BP1. J Virol. 2013; 87:9707–18. [PubMed: 23824794]

Chi X, Hadjantonakis AK, Wu Z, Hyink D, Costantini F. A transgenic mouse that reveals cell shape and arrangement during ureteric bud branching. Genesis. 2009; 47:61–6. [PubMed: 19111008]

Copley MR, Eaves CJ. Developmental changes in hematopoietic stem cell properties. Exp Mol Med. 2013; 45:e55. [PubMed: 24232254]

Costantini F, Watanabe T, Lu B, Chi X, Srinivas S. Dissection of embryonic mouse kidney, culture in vitro, and imaging of the developing organ. Cold Spring Harb Protoc. 2011 pdb prot5613.

Fazi F, Nervi C. MicroRNA: basic mechanisms and transcriptional regulatory networks for cell fate determination. Cardiovasc Res. 2008; 79:553–61. [PubMed: 18539629]

Follert P, Cremer H, Beclin C. MicroRNAs in brain development and function: a matter of flexibility and stability. Front Mol Neurosci. 2014; 7:5. [PubMed: 24570654]

Gangaraju VK, Lin H. MicroRNAs: key regulators of stem cells. Nat Rev Mol Cell Biol. 2009; 10:116–25. [PubMed: 19165214]

Ghosh T, Aprea J, Nardelli J, Engel H, Selinger C, Mombereau C, Lemonnier T, Moutkine I, Schwendimann L, Dori M, et al. MicroRNAs Establish Robustness and Adaptability of a Critical Gene Network to Regulate Progenitor Fate Decisions during Cortical Neurogenesis. Cell Rep. 2014

Guo Q, Wang Y, Tripathi P, Manda KR, Mukherjee M, Chaklader M, Austin PF, Surendran K, Chen F. Adam10 Mediates the Choice between Principal Cells and Intercalated Cells in the Kidney. J Am Soc Nephrol. 2014

Gurtan AM, Ravi A, Rahl PB, Bosson AD, JnBaptiste CK, Bhutkar A, Whittaker CA, Young RA, Sharp PA. Let-7 represses Nr6a1 and a mid-gestation developmental program in adult fibroblasts. Genes Dev. 2013; 27:941–54. [PubMed: 23630078]

Iglesias DM, Hueber PA, Chu L, Campbell R, Patenaude AM, Dziarmaga AJ, Quinlan J, Mohamed O, Dufort D, Goodyer PR. Canonical WNT signaling during kidney development. Am J Physiol Renal Physiol. 2007; 293:F494–500. [PubMed: 17494089]

Jeong HW, Jeon US, Koo BK, Kim WY, Im SK, Shin J, Cho Y, Kim J, Kong YY. Inactivation of Notch signaling in the renal collecting duct causes nephrogenic diabetes insipidus in mice. J Clin Invest. 2009; 119:3290–300. [PubMed: 19855135]

Jho EH, Zhang T, Domon C, Joo CK, Freund JN, Costantini F. Wnt/beta-catenin/Tcf signaling induces the transcription of Axin2, a negative regulator of the signaling pathway. Mol Cell Biol. 2002; 22:1172–83. [PubMed: 11809808]

Johanson TM, Skinner JP, Kumar A, Zhan Y, Lew AM, Chong MM. The role of microRNAs in lymphopoiesis. Int J Hematol. 2014

La Torre A, Georgi S, Reh TA. Conserved microRNA pathway regulates developmental timing of retinal neurogenesis. Proc Natl Acad Sci U S A. 2013; 110:E2362–70. [PubMed: 23754433]

Lee YT, de Vasconcellos JF, Yuan J, Byrnes C, Noh SJ, Meier ER, Kim KS, Rabel A, Kaushal M, Muljo SA, et al. LIN28B-mediated expression of fetal hemoglobin and production of fetal-like

erythrocytes from adult human erythroblasts ex vivo. Blood. 2013; 122:1034–41. [PubMed: 23798711]

Lize M, Klimke A, Dobbelstein M. MicroRNA-449 in cell fate determination. Cell Cycle. 2011; 10:2874–82. [PubMed: 21857159]

Ma T, Song Y, Yang B, Gillespie A, Carlson EJ, Epstein CJ, Verkman AS. Nephrogenic diabetes insipidus in mice lacking aquaporin-3 water channels. Proc Natl Acad Sci U S A. 2000; 97:4386–91. [PubMed: 10737773]

Maretto S, Cordenonsi M, Dupont S, Braghetta P, Broccoli V, Hassan AB, Volpin D, Bressan GM, Piccolo S. Mapping Wnt/beta-catenin signaling during mouse development and in colorectal tumors. Proc Natl Acad Sci U S A. 2003; 100:3299–304. [PubMed: 12626757]

Marose TD, Merkel CE, McMahon AP, Carroll TJ. Beta-catenin is necessary to keep cells of ureteric bud/Wolffian duct epithelium in a precursor state. Dev Biol. 2008; 314:112–26. [PubMed: 18177851]

Meza-Sosa KF, Pedraza-Alva G, Perez-Martinez L. microRNAs: key triggers of neuronal cell fate. Front Cell Neurosci. 2014; 8:175. [PubMed: 25009466]

Morris, JPt; Greer, R.; Russ, HA.; von Figura, G.; Kim, GE.; Busch, A.; Lee, J.; Hertel, KJ.; Kim, S.; McManus, M., et al. Dicer regulates differentiation and viability during mouse pancreatic cancer initiation. PLoS One. 2014; 9:e95486. [PubMed: 24788257]

Muzumdar MD, Tasic B, Miyamichi K, Li L, Luo L. A global double-fluorescent Cre reporter mouse. Genesis. 2007; 45:593–605. [PubMed: 17868096]

Nagalakshmi VK, Ren Q, Pugh MM, Valerius MT, McMahon AP, Yu J. Dicer regulates the development of nephrogenic and ureteric compartments in the mammalian kidney. Kidney Int. 2011; 79:317–30. [PubMed: 20944551]

Nonoguchi H, Owada A, Kobayashi N, Takayama M, Terada Y, Koike J, Ujiie K, Marumo F, Sakai T, Tomita K. Immunohistochemical localization of V2 vasopressin receptor along the nephron and functional role of luminal V2 receptor in terminal inner medullary collecting ducts. J Clin Invest. 1995; 96:1768–78. [PubMed: 7560068]

Papaioannou G, Inloes JB, Nakamura Y, Paltrinieri E, Kobayashi T. let-7 and miR-140 microRNAs coordinately regulate skeletal development. Proc Natl Acad Sci U S A. 2013; 110:E3291–300. [PubMed: 23940373]

Pastorelli LM, Wells S, Fray M, Smith A, Hough T, Harfe BD, McManus MT, Smith L, Woolf AS, Cheeseman M, et al. Genetic analyses reveal a requirement for Dicer1 in the mouse urogenital tract. Mamm Genome. 2009; 20:140–51. [PubMed: 19169742]

Patel V, Hajarnis S, Williams D, Hunter R, Huynh D, Igarashi P. MicroRNAs regulate renal tubule maturation through modulation of Pkd1. J Am Soc Nephrol. 2012; 23:1941–8. [PubMed: 23138483]

Patel V, Williams D, Hajarnis S, Hunter R, Pontoglio M, Somlo S, Igarashi P. miR-17~92 miRNA cluster promotes kidney cyst growth in polycystic kidney disease. Proc Natl Acad Sci U S A. 2013; 110:10765–70. [PubMed: 23759744]

Roush S, Slack FJ. The let-7 family of microRNAs. Trends Cell Biol. 2008; 18:505–16. [PubMed: 18774294]

Rumballe BA, Georgas KM, Combes AN, Ju AL, Gilbert T, Little MH. Nephron formation adopts a novel spatial topology at cessation of nephrogenesis. Dev Biol. 2011; 360:110–22. [PubMed: 21963425]

Sakurai H, Bush KT, Nigam SK. Heregulin induces glial cell line-derived neurotrophic growth factor-independent, non-branching growth and differentiation of ureteric bud epithelia. J Biol Chem. 2005; 280:42181–7. [PubMed: 16183643]

Shakya R, Watanabe T, Costantini F. The role of GDNF/Ret signaling in ureteric bud cell fate and branching morphogenesis. Dev Cell. 2005; 8:65–74. [PubMed: 15621530]

Short KM, Combes AN, Lefevre J, Ju AL, Georgas KM, Lamberton T, Cairncross O, Rumballe BA, McMahon AP, Hamilton NA, et al. Global quantification of tissue dynamics in the developing mouse kidney. Dev Cell. 2014; 29:188–202. [PubMed: 24780737]

Smyth GK. Linear models and empirical bayes methods for assessing differential expression in microarray experiments. Stat Appl Genet Mol Biol. 2004; 3:Article3. [PubMed: 16646809]

Sokol NS. Small temporal RNAs in animal development. Curr Opin Genet Dev. 2012; 22:368–73. [PubMed: 22578317]

Srinivas S, Watanabe T, Lin CS, William CM, Tanabe Y, Jessell TM, Costantini F. Cre reporter strains produced by targeted insertion of EYFP and ECFP into the ROSA26 locus. BMC Dev Biol. 2001; 1:4. [PubMed: 11299042]

Stohn JP, Perreault NG, Wang Q, Liaw L, Lindner V. Cthrc1, a novel circulating hormone regulating metabolism. PLoS One. 2012; 7:e47142. [PubMed: 23056600]

Subramanian A, Tamayo P, Mootha VK, Mukherjee S, Ebert BL, Gillette MA, Paulovich A, Pomeroy SL, Golub TR, Lander ES, et al. Gene set enrichment analysis: a knowledge-based approach for interpreting genome-wide expression profiles. Proc Natl Acad Sci U S A. 2005; 102:15545–50. [PubMed: 16199517]

Sugatani T, Hruska KA. Impaired micro-RNA pathways diminish osteoclast differentiation and function. J Biol Chem. 2009; 284:4667–78. [PubMed: 19059913]

Tarca AL, Draghici S, Khatri P, Hassan SS, Mittal P, Kim JS, Kim CJ, Kusanovic JP, Romero R. A novel signaling pathway impact analysis. Bioinformatics. 2009; 25:75–82. [PubMed: 18990722]

Toyoda D, Taguchi A, Chiga M, Ohmori T, Nishinakamura R. Sall4 Is Transiently Expressed in the Caudal Wolffian Duct and the Ureteric Bud, but Dispensable for Kidney Development. PLoS One. 2013; 8:e68508. [PubMed: 23825698]

Urbach A, Yermalovich A, Zhang J, Spina CS, Zhu H, Perez-Atayde AR, Shukrun R, Charlton J, Sebire N, Mifsud W, et al. Lin28 sustains early renal progenitors and induces Wilms tumor. Genes Dev. 2014; 28:971–82. [PubMed: 24732380]

Watanabe H, Yamada Y. Mice lacking link protein develop dwarfism and craniofacial abnormalities. Nat Genet. 1999; 21:225–9. [PubMed: 9988279]

Worringer KA, Rand TA, Hayashi Y, Sami S, Takahashi K, Tanabe K, Narita M, Srivastava D, Yamanaka S. The let-7/LIN-41 pathway regulates reprogramming to human induced pluripotent stem cells by controlling expression of prodifferentiation genes. Cell Stem Cell. 2014; 14:40–52. [PubMed: 24239284]

Wu CI, Shen Y, Tang T. Evolution under canalization and the dual roles of microRNAs: a hypothesis. Genome Res. 2009; 19:734–43. [PubMed: 19411598]

Wu H, Chen L, Zhou Q, Zhang X, Berger S, Bi J, Lewis DE, Xia Y, Zhang W. Aqp2-expressing cells give rise to renal intercalated cells. J Am Soc Nephrol. 2013; 24:243–52. [PubMed: 23308014]

Wulczyn FG, Smirnova L, Rybak A, Brandt C, Kwidzinski E, Ninnemann O, Strehle M, Seiler A, Schumacher S, Nitsch R. Post-transcriptional regulation of the let-7 microRNA during neural cell specification. FASEB J. 2007; 21:415–26. [PubMed: 17167072]

Yu J, Carroll TJ, McMahon AP. Sonic hedgehog regulates proliferation and differentiation of mesenchymal cells in the mouse metanephric kidney. Development. 2002; 129:5301–12. [PubMed: 12399320]

Yu J, Valerius MT, Duah M, Staser K, Hansard JK, Guo JJ, McMahon J, Vaughan J, Faria D, Georgas K, et al. Identification of molecular compartments and genetic circuitry in the developing mammalian kidney. Development. 2012; 139:1863–73. [PubMed: 22510988]

Yu J, Vodyanik MA, Smuga-Otto K, Antosiewicz-Bourget J, Frane JL, Tian S, Nie J, Jonsdottir GA, Ruotti V, Stewart R, et al. Induced pluripotent stem cell lines derived from human somatic cells. Science. 2007; 318:1917–20. [PubMed: 18029452]

Zheng W, Verlander JW, Lynch IJ, Cash M, Shao J, Stow LR, Cain BD, Weiner ID, Wall SM, Wingo CS. Cellular distribution of the potassium channel KCNQ1 in normal mouse kidney. Am J Physiol Renal Physiol. 2007; 292:F456–66. [PubMed: 16896189]

Bullet points

- The E15.5 *Dicer* mutant UB cells abnormally retained transcriptional features of the early stage UB cells
- Both principal and intercalated cell differentiation was compromised by removal of *Dicer*
- A group of genes displayed temporal expression patterns in the UB epithelium during developmental progression where their expression was detected at early developmental stages but became undetectable by E14.5
- The temporal expression pattern of early UB genes was subject to regulation by *Dicer*-dependent miRNAs
- The defect in branching morphogenesis of the *Dicer* mutant UB epithelium occurred as early as E12.5 and was cell-autonomous
- The miRNA-regulated early UB genes were enriched for *let-7* family miRNA targets
- The *let-7* family miRNAs exhibited a temporal expression pattern in the UB epithelium that is inversely correlated to that of some early UB genes including their putative targets

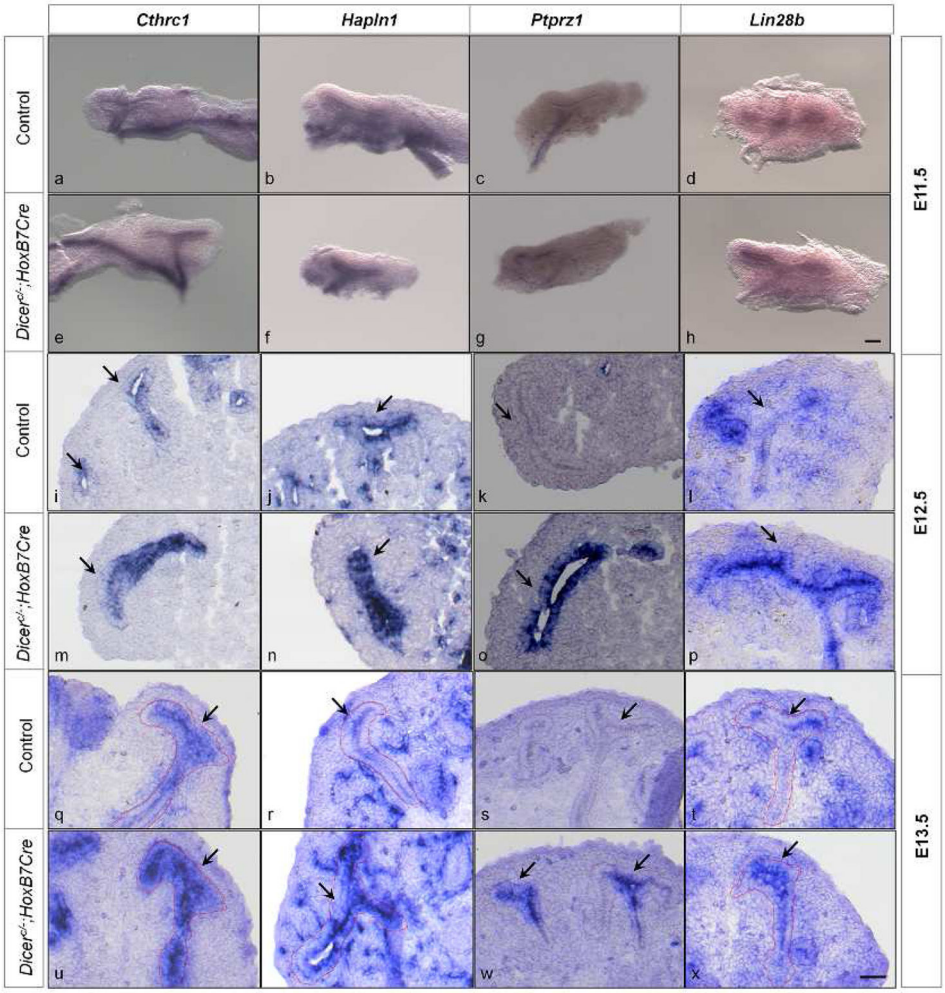

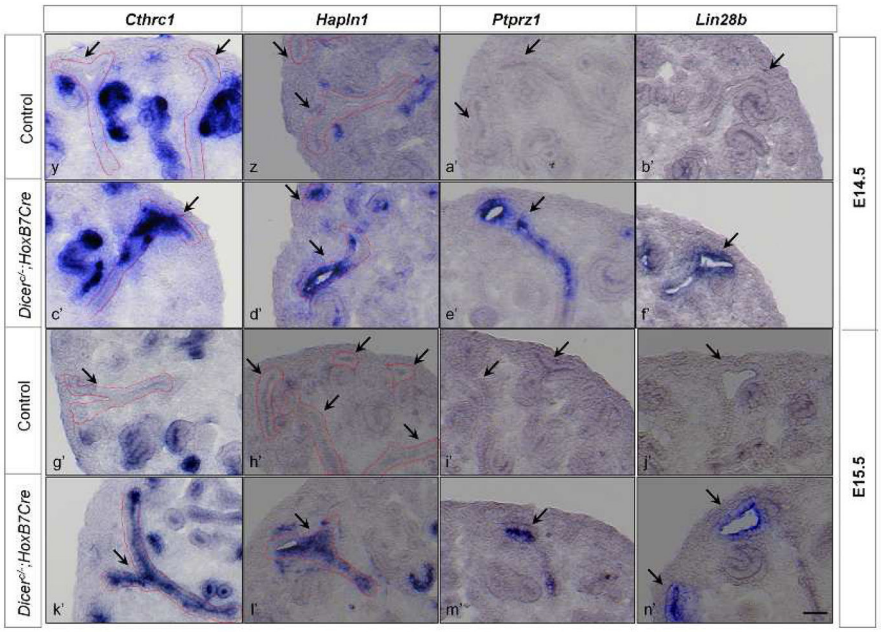

Fig. 1. miRNAs mediate temporal gene expression during UB development

In situ hybridization of *Cthrc1*, *Hapln1*, *Ptprz1*, and *Lin28b* was performed on whole-mount embryonic kidneys at E11.5 and embryonic kidney sections at E12.5–E15.5. At E11.5, all the genes are expressed in the UB epithelium of the control kidneys (a, b, c, d). At E12.5 and E13.5, except for the gene *Ptprz1* (k, s), all the genes are expressed in the UB epithelium of the control kidneys (i, j, l, q, r, t). At E14.5 and E15.5, none of the genes are detected in the UB epithelium of the control kidneys (y, z, a′, b′, g′, h′, i′, j′). Expression of *Cthrc1*, *Hapln1* and *Lin28b* is higher in the *Dicer* mutant UB epithelium at E12.5 and E13.5 (m, n, p, u, v, x) than in their control littermates, and expression in the *Dicer* mutant UB epithelium of *Cthrc1*, *Hapln1*, and *Lin28b* persists at E14.5 and E15.5 (c′, d′, f′, k′, l′, n′). Expression of *Ptprz1* persists at E12.5–E15.5 (o, w, e′, m′). Arrows point to the UB epithelium. Dotted lines also delineate the UB epithelium. Scale bar = 10 μm for panels a–h; Scale bar = 5 μm for panels i–n′.

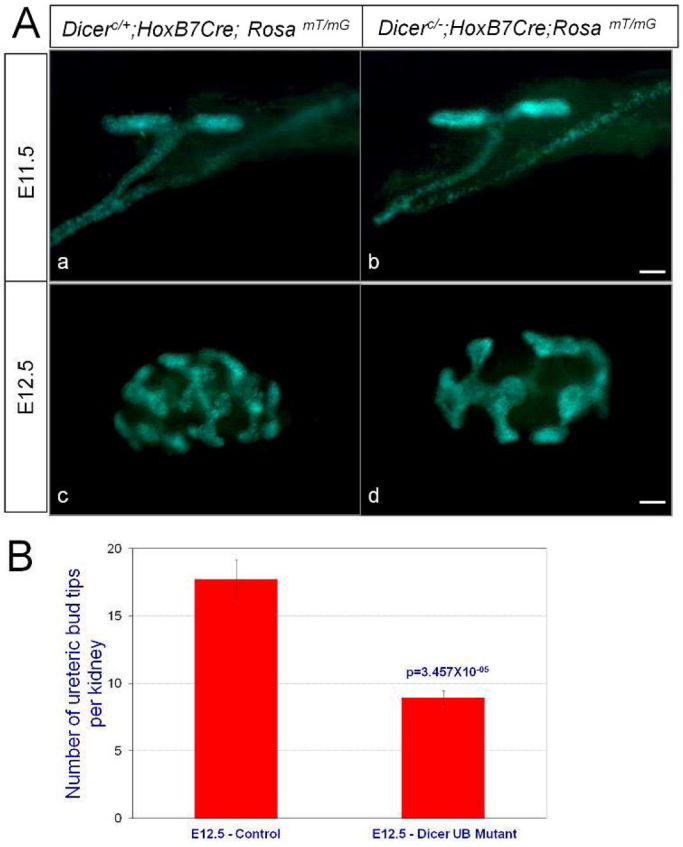

Fig. 2. Early branching defects of *Dicer* UB mutant kidneys

A. The UB epithelium was visualized with GFP fluorescence from the *Rosa*$^{mT/mG}$ Cre reporter. (a, b) Whole-mount kidneys at E11.5 exhibit no significant difference in the first branching event between the *Dicer* UB mutants (b) and their control littermates (a). (c, d) Branching of the ureteric bud epithelium of the *Dicer* UB mutants (d) is significantly reduced compared to their control littermates at E12.5. Scale bars = 10 μm. B. UB branching morphogenesis was quantified at E12.5 by measuring the number of UB tips per kidney. The number of UB tips per kidney averaged 17.75±1.44 (n=12) for the controls and 8.95±0.50 (n=19) for the *Dicer* UB mutants. Statistical significance was analyzed with Student's t-test.

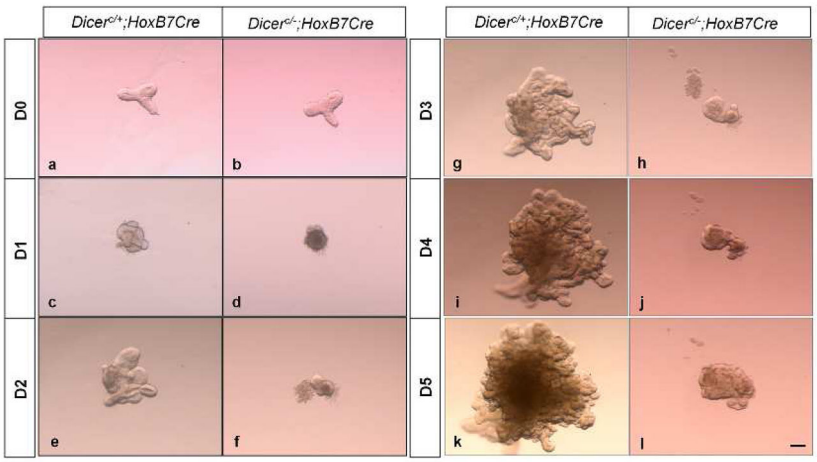

Fig. 3. Branching defect displayed by the ureteric bud epithelium of *Dicer* UB mutants is cell-autonomous and independent of the surrounding metanephric mesenchyme

Isolated ureteric buds from E11.5 *Dicer* mutants (b) and control littermates (a) showed no significant difference at the point of dissection. On culturing in Matrigel supplemented with Gdnf and retinoic acid, the mutant ureteric buds (d, f, h, j, l) displayed a significant reduction in branching compared to ureteric buds derived from kidneys of control littermates (c, e, g, i, k) as early as 24 h in the culture (d). Scale bar =10 μm.

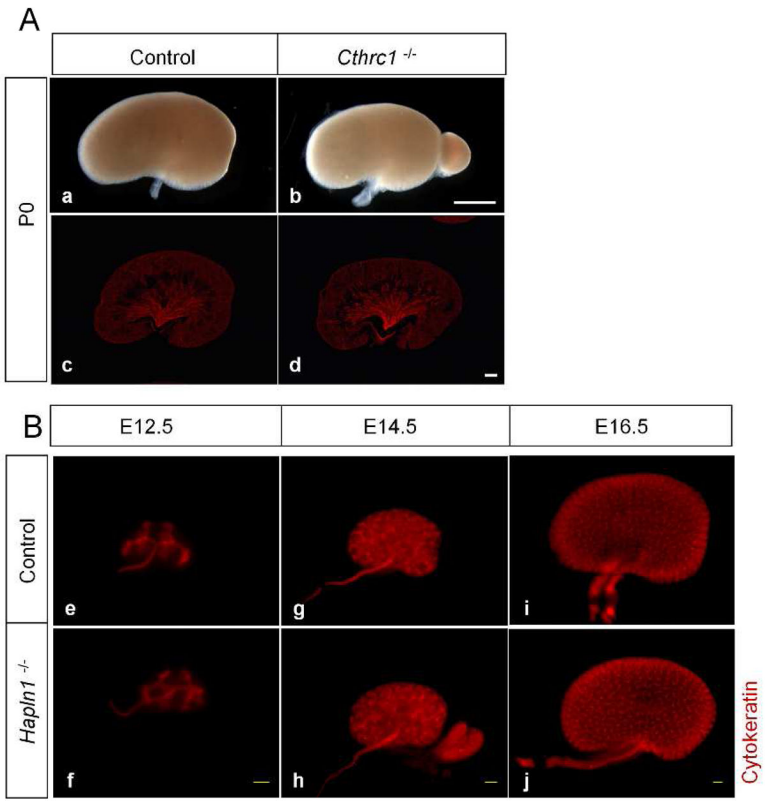

Fig. 4. Branching morphogenesis is unaffected in the ureteric bud epithelium of *Cthrc1* and *Hapln1 (Crtln1)* null mutant kidneys

Immunostaining with anti-pan cytokeratin on P0 kidney sections of *Cthrc1* null mutants (A) and whole-mount kidneys of E12.5, E14.5, and E16.5 *Hapln1* null mutants (B) reveals no significant difference in branching morphogenesis in the mutants (d, f, h, j) compared with their respective control littermates (c, e, g, i). Scale bar=100 μm for all panels in A; scale bar=10 μm for all panels in B.

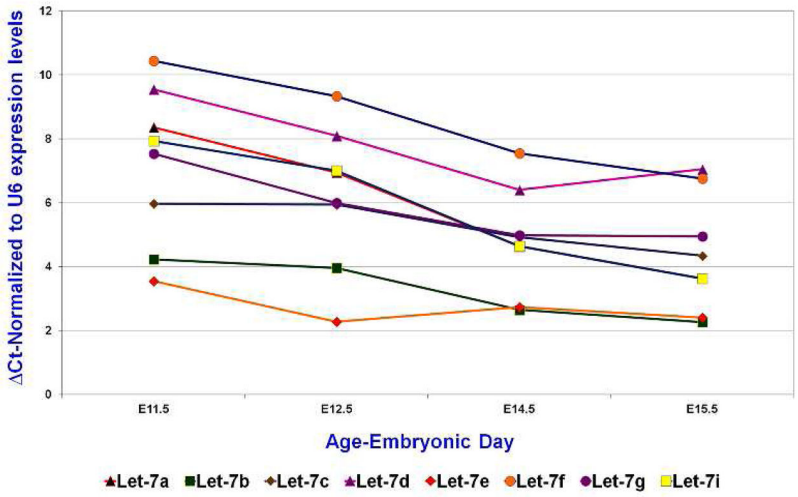

Fig. 5. Temporal expression profiles of the *let-7* family miRNAs in the ureteric bud epithelium during kidney development

qRT-PCR examination of *let-7* family miRNA expression in isolated mesenchyme-free ureteric buds (E11.5) and FACS-sorted ureteric bud epithelial cells (E12.5–E15.5). Note that a higher C_t indicates a lower amount of miRNAs.

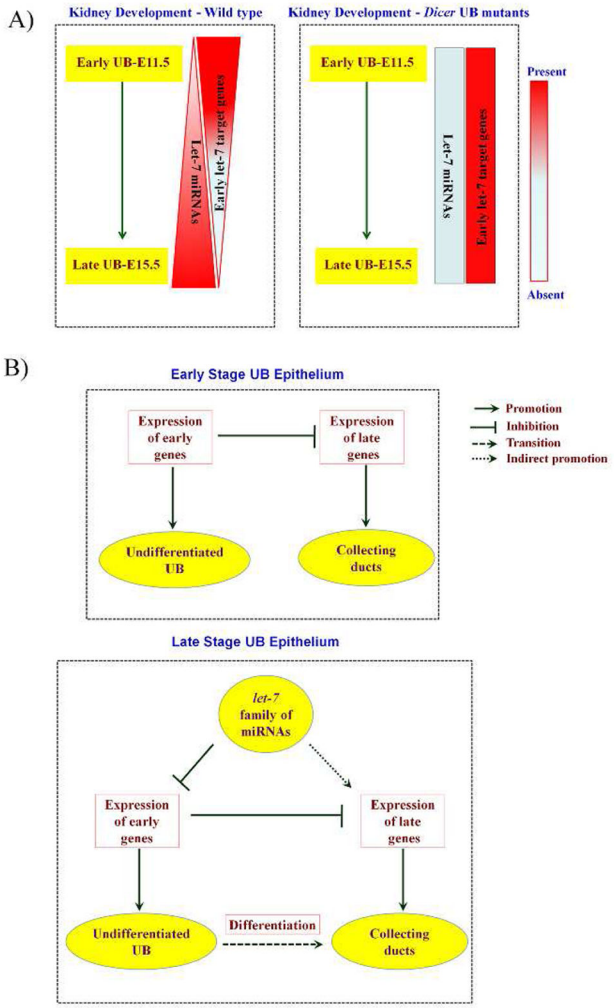

Fig. 6. A summary and a model for *let-7* family miRNA-regulated gene expression in UB epithelial cell fate changes promoting collecting duct differentiation

A) During UB epithelial development, the *let-7* family of miRNAs exhibits a temporally regulated gene expression pattern which is inversely correlated with the temporal expression pattern of putative early UB *let-7* target genes. This temporal expression pattern of the *let-7* family miRNAs and their targets is altered in the *Dicer* mutant UB epithelium, where the expression of the *let-7* family miRNAs is disrupted, and the expression of early *let-7* targets persists in the later stages of UB epithelial morphogenesis. B) During normal kidney development, the expression of early UB genes at early developmental stages defines the undifferentiated UB epithelium and inhibits the expression of late genes (collecting duct differentiation genes). At later developmental stages, the *let-7* family miRNAs, directly or through their target genes, inhibit the expression of some of the early UB genes, thereby facilitating the expression of late genes in the UB epithelium, and this late gene expression defines the collecting duct fate.

Table 1

E10.5 ureteric bud epithelial genes (Gudmap kidney e10.5 UretericTip HoxB7 1000, Source: Gudmap Mouse MOE430.2) enriched (p Value= 4.859×10^{-17}) in the up-regulated transcripts of the E15.5 *Dicer* mutant ureteric bud epithelium (n=679 genes; FC ≥1.5; p Value ≤ 0.05) based on the ToppGene analysis.

	Gene Symbol	Fold change
1	*Hapln1*	15.8
2	*Prtg*	7.0
3	*Cthrc1*	5.8
4	*Ptprz1*	5.2
5	*Scd*	3.5
6	*Ednrb*	3.4
7	*Clcn5*	3.1
8	*Polr3g*	3.1
9	*Lin28b*	3.0
10	*Igf2bp1*	2.7
11	*Cdkn1a*	2.6
12	*Syt11*	2.6
13	*Slc16a1*	2.5
14	*Sytl5*	2.4
15	*Pkhd1*	2.3
16	*Fli1*	2.3
17	*Endod1*	2.3
18	*Pcdh7*	2.2
19	*Mfsd6*	2.2
20	*Susd1*	2.2
21	*Gria3*	2.1
22	*Lrp2*	2.1
23	*Fign*	2.0
24	*Polq*	2.0
25	*Fjx1*	2.0
26	*Pde3b*	1.9
27	*Galnt3*	1.9
28	*Gpr15*	1.9
29	*Gldc*	1.9
30	*E2f5*	1.9
31	*Dusp9*	1.9
32	*Tmem30b*	1.8
33	*Tnfaip6*	1.8
34	*Ssh2*	1.8
35	*Hook1*	1.8
36	*Tmem59l*	1.8
37	*Chd7*	1.8

	Gene Symbol	Fold change
38	*Il17rd*	1.8
39	*Gng3*	1.7
40	*Ccdc80*	1.7
41	*Nrbp1*	1.7
42	*Eml5*	1.7
43	*En2*	1.7
44	*Kbtbd8*	1.7
45	*Rab30*	1.6
46	*Tubb2b*	1.6
47	*Dpp4*	1.6
48	*Tmtc2*	1.6
49	*Kcnj16*	1.6
50	*Bmp5*	1.6
51	*Rnmt*	1.6
52	*Brwd3*	1.6
53	*Slain1*	1.6
54	*Tgfbr1*	1.6
55	*Baz1a*	1.5
56	*Ankrd45*	1.5
57	*Gja1*	1.5
58	*Dkk1*	1.5
59	*Cecr2*	1.5
60	*Thap2*	1.5
61	*Ccnj*	1.5
62	*Ly75*	1.5
63	*Hmcn1*	1.5
64	*Ddx3x*	1.5

Table 2

E15.5 medullary collecting duct genes (Gudmap developing Kidney e15.5 Medullary collecting duct 1000 k1, Source: Gudmap Mouse MOE430.2) enriched (p Value = 2.390×10^{-25}) in the down-regulated transcripts of the E15.5 *Dicer* mutant ureteric bud epithelium (n=440 genes; FC ≤ −1.5; p Value ≤ 0.05) based on the ToppGene analysis.

	Gene Symbol	Fold change
1	*Sprr1a*	−4.5
2	*Upk1b*	−3.2
3	*Adh1c*	−2.9
4	*Ctse*	−2.8
5	*Muc20*	−2.5
6	*Snx31*	−2.5
7	*Upk3a*	−2.5
8	*Slc16a5*	−2.4
9	*Avpr2*	−2.3
10	*Pdzk1ip1*	−2.3
11	*Krt19*	−2.3
12	*Ptges*	−2.2
13	*Tspan8*	−2.1
14	*Gsdmc*	−2.0
15	*Ptgs1*	−1.9
16	*Fxyd3*	−1.9
17	*Fxyd4*	−1.9
18	*Degs2*	−1.8
19	*Mal*	−1.8
20	*Pllp*	−1.8
21	*S100a6*	−1.8
22	*Pycard*	−1.8
23	*Pof1b*	−1.7
24	*Lypd6b*	−1.7
25	*Aqp3*	−1.7
26	*Rnf186*	−1.7
27	*Pparg*	−1.7
28	*Btc*	−1.7
29	*Ehf*	−1.7
30	*Foxa1*	−1.6
31	*Ppp1r3c*	−1.6
32	*Sh2d4a*	−1.6
33	*Tmem117*	−1.6
34	*Dab1*	−1.6
35	*Rap1gap*	−1.6
36	*Kcnq1*	−1.5

	Gene Symbol	Fold change
37	*Il17re*	−1.5
38	*Lypd6*	−1.5

Table 3

ToppGene analysis showing the enrichment of *let-7* miRNA regulation of genes in Table 1. Note ToppGene used the human *let-7* miRNA sequences which share the mature miRNA sequences with the mouse homologs.

	Name	Source	p-Value
1	hsa-let-7a	TargetScan	9.74×10^{-9}
2	hsa-let-7b	TargetScan	9.74×10^{-9}
3	hsa-let-7c	TargetScan	9.74×10^{-9}
4	hsa-let-7d	TargetScan	9.74×10^{-9}
5	hsa-let-7e	TargetScan	9.74×10^{-9}
6	hsa-let-7f	TargetScan	9.74×10^{-9}
7	hsa-let-7g	TargetScan	9.74×10^{-9}
8	hsa-let-7i	TargetScan	9.74×10^{-9}
9	hsa-miR-98	TargetScan	9.74×10^{-9}
7	hsa-let-7a	PITA	4.67×10^{-7}
8	hsa-let-7b	PITA	4.67×10^{-7}
9	hsa-let-7c	PITA	4.67×10^{-7}
10	hsa-let-7d	PITA	4.67×10^{-7}
11	hsa-let-7e	PITA	4.67×10^{-7}
12	hsa-let-7f	PITA	4.67×10^{-7}
13	hsa-let-7g	PITA	4.67×10^{-7}
14	hsa-let-7i	PITA	4.67×10^{-7}
15	hsa-miR-98	PITA	4.35×10^{-6}

Table 4

Genes in Table 1 that are predicted to be *let-7* family miRNA targets by the ToppGene analysis and the miRWalk analysis.

	Gene Symbol	Fold change	miRWalk-predicted *LET-7* miRNAs regulating the gene
1	*Prtg*	7.0	*mmu-let-7a; 7b; 7c; 7d; 7e; 7f; 7g; 7i*
2	*Cthrc1*	5.8	*mmu-let-7a; 7b; 7c; 7d; 7e; 7f; 7g; 7i*
3	*Scd*	3.5	*mmu-let-7a; 7b; 7c; 7d; 7e; 7f; 7g; 7i*
4	*Clcn5*	3.1	No predicted *let-7* miRNA target sites for mouse *Clcn5* gene
5	*Lin28b*	3.0	*mmu-let-7a; 7b; 7c; 7d; 7e; 7f; 7g; 7i*
6	*Igf2bp1*	2.7	*mmu-let-7a; 7b; 7c; 7d; 7e; 7f; 7g; 7i*
7	*Cdkn1a*	2.6	No predicted *let-7* miRNA target sites for mouse *Cdkn1a* gene
8	*Syt11*	2.6	*mmu-let-7a; 7b; 7c; 7d; 7e; 7f; 7g; 7i*
9	*Fign*	2.0	*mmu-let-7a; 7b; 7c; 7d; 7e; 7f; 7g; 7i*
10	*E2f5*	1.9	*mmu-let-7a; 7b; 7c; 7d; 7e; 7f; 7g; 7i*
11	*Dusp9*	1.9	*mmu-let-7a; 7b; 7c; 7d; 7e; 7f; 7g; 7i*
12	*Hook1*	1.8	*mmu-let-7a; 7b; 7c; 7d; 7e; 7f; 7g; 7i*
13	*Chd7*	1.8	*mmu-let-7a; 7b; 7c; 7e; 7f; 7g; 7i*
14	*Tgfbr1*	1.6	*mmu-let-7a; 7b; 7c; 7d; 7e; 7f; 7g; 7i*
15	*Ly75*	1.5	No predicted *let-7* miRNA target sites for mouse *Ly75* gene
16	*Ccnj*	1.5	*mmu-let-7a; 7b; 7c; 7d; 7e; 7f; 7g; 7i*

Table 5

The *LET-7* miRNA family members expressed in the E15.5 ureteric bud epithelium with the miRNA microarray analysis.

	Average Signal Intensity (2 replicates)	Mature miRNA sequence
mmu-let-7g	258	UGAGGUAGUAGUUUGUACAGUU
mmu-let-7f	636	UGAGGUAGUAGAUUGUAUAGUU
mmu-let-7b	1,545	UGAGGUAGUAGGUUGUGUGGUU
mmu-let-7e	1,686	UGAGGUAGGAGGUUGUAUAGUU
mmu-let-7c	1,905	UGAGGUAGUAGGUUGUAUGGUU
mmu-let-7a	2,038	UGAGGUAGUAGGUUGUAUAGUU
mmu-let-7d	2,848	AGAGGUAGUAGGUUGCAUAGUU
mmu-let-7i	3,142	UGAGGUAGUAGUUUGUGCUGUU